# Nitrogen-15-Labeled Oligodeoxynucleotides. 4. Tetraplex Formation of d[G($^{15}$N$^{7}$)GTTTTTGG] and d[T($^{15}$N$^{7}$)GGGT] Monitored by $^{1}$H Detected $^{15}$N NMR

**Barbara L. Gaffney, Chuan Wang, and Roger A. Jones***

*Contribution from the Department of Chemistry, Rutgers, The State University of New Jersey, Piscataway, New Jersey 08855.* *Received August 21, 1991*

**Abstract:** We have synthesized two molecules containing [7-$^{15}$N]-labeled 2′-deoxyguanosine, d[G($^{15}$N$^{7}$)GTTTTTGG], and d[T($^{15}$N$^{7}$)GGGT] which, under appropriate conditions, will form tetramolecular complexes. The $^{15}$N chemical shifts of these molecules and of their Watson–Crick duplexes, d[G($^{15}$N$^{7}$)GTTTTTGG]·d[CCAAAAACC] and d[T($^{15}$N$^{7}$)GGGT]·d[ACCCA], were monitored as a function of temperature. The $^{15}$N chemical shift of the labeled N7 atom in each tetramolecular complex shows a similar temperature dependence, and the chemical shifts are not signal-averaged. The similarity of the chemical shifts for the tetraplex and single strand structures, and the difference seen for the two duplexes, are consistent with the different degrees of hydrogen bonding to the N7 which could be expected in each case. Thus, although more examples will be required to establish the generality of these observations, a purine [7-$^{15}$N] label appears to be able to monitor major groove interactions, including hydration.

The $^{15}$N chemical shifts of the nucleic acid nitrogen atoms involved in Watson–Crick hydrogen bonding have proved to be sensitive monitors of base-pairing, both in monomer studies and in studies of nucleic acid fragments.[1-8] In addition, the chemical shift of a [1-$^{15}$N]adenine in two DNA duplexes recently was used to demonstrate protonation of the adenine N1 in either an A·C or an A·G mispair.[9] The purine N7 atom, which is not involved in Watson–Crick H-bonding, instead has the potential to monitor major groove interactions. In particular, the Hoogsteen H-bonding proposed in triple helices[10-14] and in guanine tetrads[15-18] as well as ligand interactions ranging from protein binding[19] to hydration could be probed by appropriate [7-$^{15}$N]-labeled molecules. We recently have developed a route for synthesis of [7-$^{15}$N]-2′-deoxyguanosine[20] and have now prepared two [7-$^{15}$N]-labeled oligodeoxynucleotides, d[G($^{15}$N$^{7}$)GTTTTTGG] (**1**) and d[T-($^{15}$N$^{7}$)GGGT] (**2**). Each of these molecules (unlabeled) has been shown to form, under appropriate conditions, a tetramolecular complex.[21,22] The $^{15}$N chemical shifts of these molecules and of their Watson–Crick duplexes with, respectively, d-[CCAAAAACC] (**3**) and d[ACCCA] (**4**), were monitored as a function of temperature using a $^{1}$H-detected heteronuclear 2D NMR experiment.[9,23]

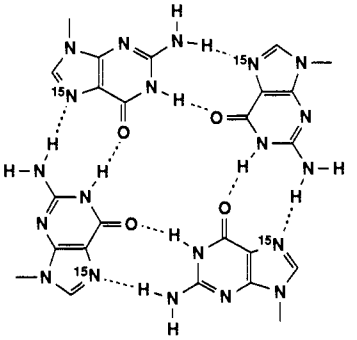

The syntheses of **1**, **2**, and **4** were carried out by an H-phosphonate method, on scales of 15–34 μmol.[9,24,25] The synthesis of **3** by a phosphoramidite method has been reported previously.[26] Each molecule was purified by reversed-phase HPLC both before and after detritylation, and each was characterized by enzymatic degradation to its constituent deoxynucleosides.[26]

**{d[G($^{15}$N$^{7}$)GTTTTTGG]}$_4$ and d[G($^{15}$N$^{7}$)GTTTTTGG]·d-[CCAAAAACC].** The $^{15}$N chemical shifts of the N7 atom of **1** in 0.1 M sodium and in the presence and absence of its Watson–Crick complement **3** are listed in Tables I and II and are plotted in Figure 1. At 80°, where both samples are dissociated to the single strands, the chemical shifts converge to single resonances at about 216.0 ppm. As the temperature is lowered, tetraplex or duplex formation first results in opposite changes in chemical shift for the two samples. At 0°, where the samples are predominantly associated to the tetraplex and duplex forms, the tetraplex chemical shift is approximately 1.5 ppm upfield of the duplex chemical shift. At intermediate temperatures the two samples show quite different behavior. The duplex sample gives one signal averaged resonance, as we have seen previously for the adenine N1 in other duplexes.[6,8] In contrast, the tetraplex sample

(1) Poulter, C. D.; Livingston, C. L. *Tetrahedron Lett.* **1979**, *9*, 755–758.
(2) Dyllick-Brenzinger, C.; Sullivan, G. R.; Pang, P. P.; Roberts, J. D. *Proc. Natl. Acad. Sci. U.S.A.* **1980**, *77*, 5580–5582.
(3) James, T. L.; James, J. L.; Lapidot, A. *J. Am. Chem. Soc.* **1981**, *103*, 6748–6750.
(4) Griffey, R. H.; Poulter, D. D. *Tetrahedron Lett.* **1983**, *24*, 4067–4070.
(5) Kanamori, K.; Roberts, J. D. *Acc. Chem. Res.* **1983**, *16*, 35–41.
(6) Gao, X.; Jones, R. A. *J. Am. Chem. Soc.* **1987**, *109*, 3169–3171.
(7) Buchanan, G. W. *Tetrahedron* **1989**, *45*, 581–604.
(8) Wang, C.; Gao, X.; Jones, R. A. *J. Am. Chem. Soc.* **1991**, *113*, 1448–1450.
(9) Wang, C.; Gao, H.; Gaffney, B. L.; Jones, R. A. *J. Am. Chem. Soc.* **1991**, *113*, 5486–5488.
(10) Felsenfeld, G.; Davies, D. R.; Rich, A. *J. Am. Chem. Soc.* **1957**, *79*, 2023–2024.
(11) Riley, M.; Maling, B.; Chamberlin, M. J. *J. Mol. Biol.* **1966**, *20*, 359–389.
(12) Morgan, A. R.; Wells, R. D. *J. Mol. Biol.* **1968**, *37*, 63–80.
(13) Mirkin, S. M.; Lyamichev, V. I.; Drushlyak, K. N.; Dobrynin, V. N.; Filippov, S. A.; Frank-Kamenetskii, M. D. *Nature (London)* **1987**, *330*, 495–497.
(14) Moser, H. E.; Dervan, P. B. *Science* **1987**, *238*, 645–650.
(15) Sen, D.; Gilbert, W. *Nature (London)* **1988**, *334*, 364–366.
(16) Sundquist, W. I.; Klug, A. *Nature (London)* **1989**, *342*, 825–829.
(17) Williamson, J. R.; Raghuraman, M. K.; Cech, T. R. *Cell* **1989**, *59*, 871–880.
(18) Panyutin, I. G.; Kovalsky, O. I.; Budowsky, E. I.; Dickerson, R. E.; Rikhirev, M. E.; Lipanov, A. A. *Proc. Natl. Acad. Sci. U.S.A.* **1990**, *87*, 867–870.
(19) Massefski, W., Jr.; Redfield, A.; Sarma, U. D.; Bannerji, A.; Roy, S. *J. Am. Chem. Soc.* **1990**, *112*, 5350–5351.
(20) Gaffney, B. L.; Kung, P.-P.; Jones, R. A. *J. Am. Chem. Soc.* **1990**, *112*, 6748–6749.
(21) Jin, R.; Breslauer, K. J.; Jones, R. A.; Gaffney, B. L. *Science* **1990**, *250*, 543–546.
(22) Jin, R.; Gaffney, B. L.; Wang, C.; Breslauer, K. J.; Jones, R. A., manuscript in preparation.
(23) Bodenhausen, G.; Ruben, D. J. *Chem. Phys. Lett.* **1980**, *69*, 185–189.
(24) Gaffney, B. L.; Jones, R. A. *Tetrahedron Lett.* **1988**, *29*, 2619–2622.
(25) Gao, H.; Gaffney, B. L.; Jones, R. A. *Tetrahedron Lett.* **1991**, *32*, 5477–5480.
(26) Gaffney, B. L.; Jones, R. A. *Biochemistry* **1989**, *28*, 5881–5889.

0002-7863/92/1514-4047$03.00/0 

**Table I.** Chemical Shifts and Relative Intensities[a] of the Resonances Observed for d[G($^{15}$N$^{7}$)GTTTTTGG]

| temp, °C | tetraplex form δ (ppm) | intensity,[a] % | single strand δ (ppm) | intensity,[a] % | minor form δ (ppm) | intensity,[a] % |
|---|---|---|---|---|---|---|
| 0.0 | 214.7 | 100 | | | | |
| 5.0 | 214.8 | 100 | | | | |
| 10.0 | 215.0 | 80 | | | 216.0 | 20 |
| 15.0 | 215.1 | 63 | 214.9 | 10 | 216.0 | 27 |
| 20.0 | 215.3 | 67 | 215.0 | 9 | 216.0 | 24 |
| 25.0 | 215.4 | 60 | 215.0 | 14 | 216.1 | 26 |
| 30.0 | 215.5 | 53 | 215.2 | 26 | 216.2 | 21 |
| 35.0 | 215.7 | 30 | 215.2 | 70 | | |
| 40.0 | | | 215.4 | 100 | | |
| 45.0 | | | 215.5 | 100 | | |
| 60.0 | | | 215.7 | 100 | | |
| 80.0 | | | 216.1 | 100 | | |

[a] The relative intensities are based on peak heights and have an estimated error or ±10%.

**Table II.** Chemical Shifts Observed for d[G($^{15}$N$^{7}$)GTTTTTGG]·d[AACCCCCAA]

| temp, °C | duplex/single strand δ (ppm) | temp, °C | duplex/single strand δ (ppm) |
|---|---|---|---|
| 0 | 216.2 | 60 | 216.3 |
| 20 | 216.9 | 80 | 216.0 |
| 40 | 217.3 | | |

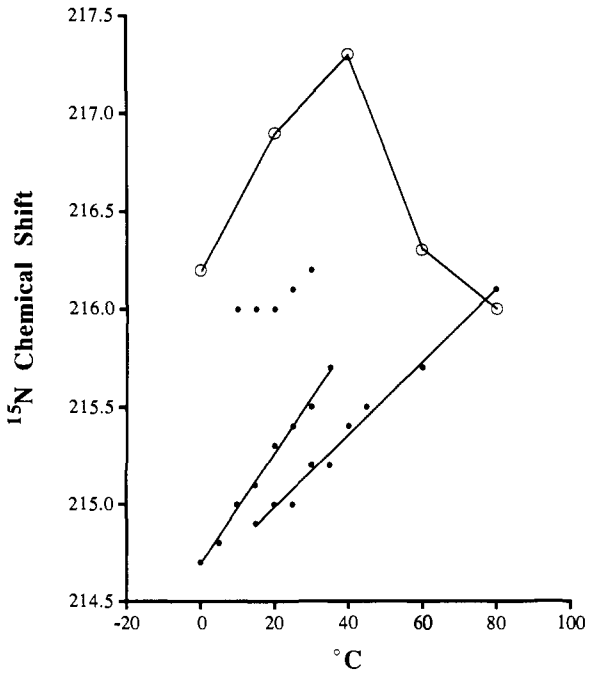


**Figure 1.** Plot of the $^{15}$N chemical shifts of d[G($^{15}$N$^{7}$)GTTTTTGG] (10.1 mM), solid circles, and d[G($^{15}$N$^{7}$)GTTTTTGG]·d-[CCAAAAACC] (7.8 mM), open circles, in $D_2O$ containing 0.1 M NaCl, 10 mM phosphate, 0.1 mM EDTA at pH 6.9 or 7.0, respectively, over a temperature range of 0–80 °C. The $^{15}$N chemical shifts are relative to $^{15}NH_4Cl$ in 10% HCl. The data were obtained by using an antiphase version of the heteronuclear single quantum correlation experiment:[23] $90°(H_x) - 1/(4\,^2J_{NH}) - 180°(H), 180°(N) - 1/(4\,^2J_{NH}) - 90°(H_y), 90°(N_{\pm x}) - t_1/2 - 180°(H) - t_1/2 - 90°(H_x), 90°(N_x)$ – acq-(±). The spectra were recorded at a $^1$H frequency of 500 MHz with a resolution of 0.3 ppm/point for the $^{15}$N dimension. Two to four transients for each FID were acquired at a total acquisition time of 4–8 min. The error is estimated to be ± 0.3 ppm.

shows separate resonances for the single strand, the tetraplex, and an unidentified minor form which is also visible in the $^1$H NMR.[27] As the temperature is increased the relative intensities of the tetraplex and single strand resonances invert (Table I), while both chemical shifts show a linear downfield drift. The duplex sample shows a similar downfield drift until the duplex begins to dissociate

(27) Wang, Y.; Jin, R.; Gaffney, B. L.; Jones, R. A.; Breslauer, K. J. *Nucleic Acids Res.* **1991**, *19*, 4619–4622.

**Table III.** Chemical Shifts and Relative Intensities[a] of the Resonances Observed for d[T($^{15}$N$^{7}$)GGGT]

| temp, °C | tetraplex form δ (ppm) | intensity,[a] ‰ | single strand δ (ppm) | intensity,[a] % |
|---|---|---|---|---|
| 0 | 214.9 | 90 | 214.3 | 10 |
| 15 | 215.4 | 90 | 214.8 | 10 |
| 30 | 216.0 | 90 | 215.1 | 10 |
| 45 | 216.6 | 60 | 215.4 | 40 |
| 60 | | | 215.7 | 100 |
| 80 | | | 216.2 | 100 |

[a] The relative intensities are based on peak heights and have an estimated error of ±10%.

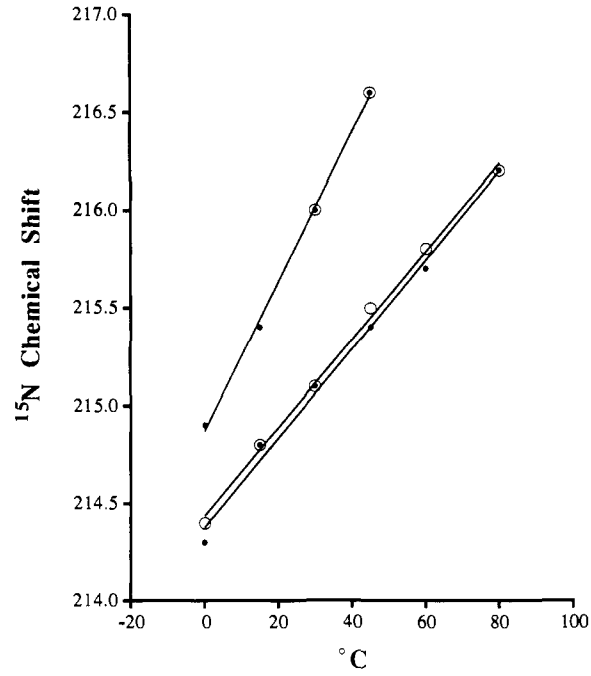


**Figure 2.** Plot of the $^{15}$N chemical shifts of d[T($^{15}$N$^{7}$)GGGT] (5.0 mM), solid circles, and d[T($^{15}$N$^{7}$)GGGT]·d[ACCCA] (9.0 mM), open circles, in $D_2O$ containing 16 mM potassium ion, 10 mM phosphate, 0.2 mM EDTA at pH 7.0, over a temperature range of 0–80 °C. The conditions were as described in Figure 1.

at about 40°, whereupon the chemical shift changes dramatically, moving back upfield because of signal averaging with the single strand.

**{d[T($^{15}$N$^{7}$)GGGT]}$_4$ and d[T($^{15}$N$^{7}$)GGGT]·d[ACCCA].** The $^{15}$N chemical shifts of the N7 atom of **2** in 16 mM potassium and in the presence and absence of its Watson–Crick complement **4** are listed in Tables III and IV and are plotted in Figure 2. Once again, at 80° each sample shows a single resonance at the same chemical shift, again near 216 ppm. As the temperature is lowered, the tetraplex sample (**2**) behaves much like **1**, although 10% of the single strand remains even at 0°. The duplex sample, however, does not behave analogously to the **1·3** duplex. Instead,

**Table IV.** Chemical Shifts and Relative Intensities[a] of the Resonances Observed for d[T($^{15}$N$^7$)GGGT]·d[ACCCA]

| temp, °C | duplex/single strand δ (ppm) | intensity,[a] % | tetraplex form δ (ppm) | intensity,[a] % |
|---|---|---|---|---|
| 0 | 214.4 | 100 | | |
| 15 | 214.8 | 100 | | |
| 30 | 215.1 | 83 | 216.0 | 17 |
| 45 | 215.5 | 80 | 216.6 | 20 |
| 60 | 215.8 | 100 | | |
| 80 | 216.2 | 100 | | |

[a] The relative intensities are based on peak heights and have an estimated error of ±10%.

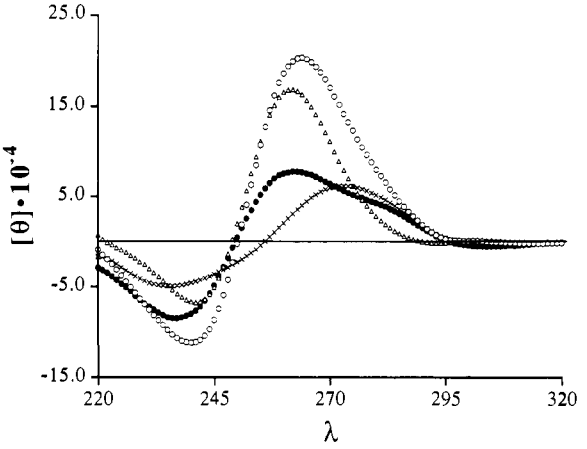


**Figure 3.** Circular dichroism spectra at 0 °C in 16 mM potassium ion, 10 mM phosphate, 0.1 mM EDTA at pH 7.2 of "△" d[TGGGT] (**2**), 15.3 × 10$^{-6}$ M; "x" d[ACCCA] (**4**), 19.1 × 10$^{-6}$ M; "○" sum of the spectra of **2** and **4**; "●" d[TGGGT]·d[ACCCA] (**2·4**), 11.4 × 10$^{-6}$ M in total strands. Each spectrum is the smoothed average of two scans from which the buffer background was subtracted. The spectra were normalized to a concentration of 10$^{-5}$ M in each single strand present.

the **2·4** sample shows only resonances with the same chemical shifts seen with **2** alone, although the relative intensities are very different (Tables III and IV). For example, at 30° the sample of **2** shows relative intensities of about 10% for the 215.1 ppm resonance (single strand) and 90% for the 216.0 ppm resonance (tetraplex), while the **2·4** sample shows intensities of 83% for the resonance at 215.1 ppm and 17% at 216.0 ppm. If the **2·4** sample is predominantly in the duplex form at low temperature, these results would indicate that the $^{15}$N chemical shift for the labeled N7 atom must be identical for both the duplex and the single strand, for this molecule.

The extent of duplex formation in both the **1·3** and **2·4** samples is indicated qualitatively by their CD and $^1$H NMR spectra. Specifically, the CD spectra shown in Figures 3 and 4 demonstrate in each case the presence of a structure in the duplex samples that is not present in the separate single strand samples, since the duplex spectra are not simply the sum of the single strand spectra. Furthermore, the $^1$H NMR spectra of the duplex samples, determined in $H_2O$ (Figures 5 and 6), both show resonances between 12.5 and 14.5 that are characteristic of duplex formation. In addition, in the **2·4** sample, but not in the **1·3** sample, there remain some resonances from the tetraplex form. Note that because of the $H_2O$ suppression required to obtain these spectra, the relative intensities of the duplex and tetraplex resonances observed in Figure 5 cannot be used to determine the relative amounts of each species present. However, the amount of tetraplex in the **2·4** sample, at low temperature, must be very small since it is not detectable in the heteronuclear 2D spectra of this sample until temperatures where the duplex is likely to be substantially dissociated. Further, since at low temperature the sample of **2** alone contains only 10% of the single strand (Table III), it follows that the amount of single strand present in the **2·4** sample, at low temperature, should be not more than, and probably is less than, 10% of the amount of tetraplex present. Thus, we conclude that the duplex samples contain little or no single strand at low temperature, and therefore that the $^{15}$N chemical shifts for the **2·4** duplex and the single strand form of **2** are identical and fall on the same line in Figure 2.

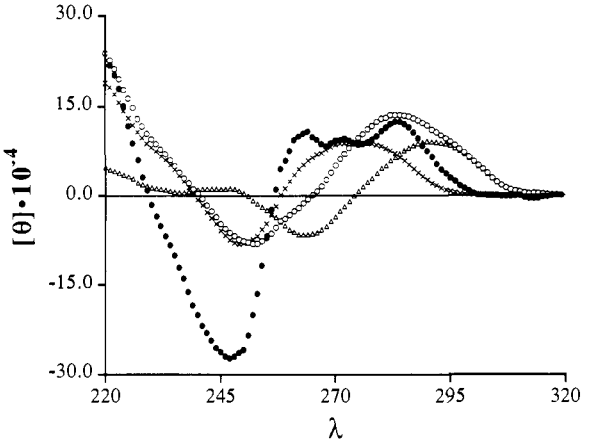


**Figure 4.** Circular dichroism spectra at 0 °C in 0.1 M NaCl, 10 mM phosphate, 0.2 mM EDTA at pH 7.2 of "△" d[GGTTTTTGG] (**1**), 13.2 × 10$^{-6}$ M; "x" d[CCAAAAACC] (**3**), 12.9 × 10$^{-6}$ M; "○" sum of the spectra of **1** and **3**; "●" d[GGTTTTTGG]·d[CCAAAAACC] (**1·4**), 15.6 × 10$^{-6}$ M in total strands. Each spectrum is the smoothed average of two scans from which the buffer background was subtracted. The spectra were normalized to a concentration of 10$^{-5}$ M in each single strand present.

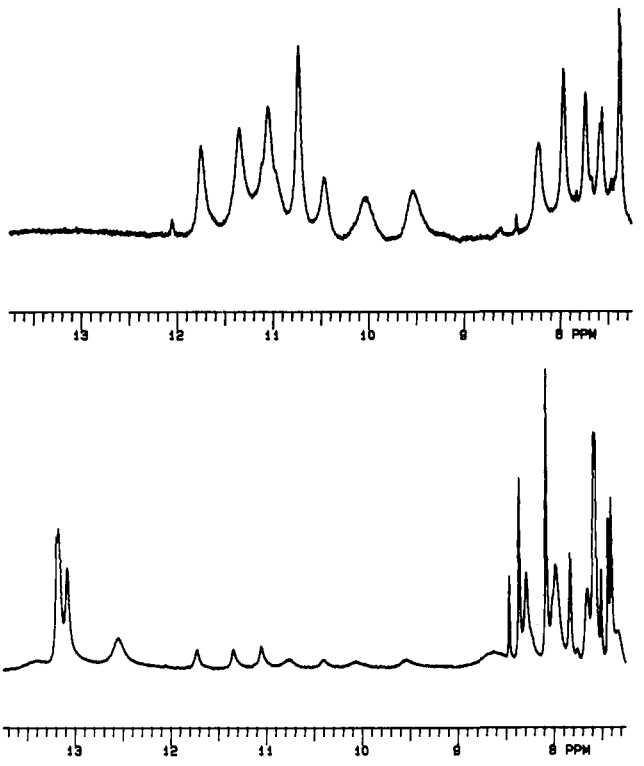


**Figure 5.** The 400-MHz $^1$H NMR spectra at 3 °C of, upper, d[T($^{15}$N$^7$)GGGT] (5.0 mM) and, lower, d[T($^{15}$N$^7$)GGGT]·d[ACCCA] (9.0 mM), in $H_2O/D_2O$ (9:1) containing 16 mM potassium ion, 10 mM phosphate, 0.2 mM EDTA at pH 7.0.

## Discussion

Hydrogen bonding to an sp$^2$ nitrogen is expected to result in an upfield shift of the nitrogen resonance, as has been observed for Watson–Crick H-bonding.[1-9,19] Furthermore, the N7 of guanosine-5′-monophosphate in water resonates 12.6 ppm upfield of its position in dimethyl sulfoxide.[28] In the experiments reported here at least two fundamentally different types of H-bonding to

(28) Markowski, V.; Sullivan, G.; Roberts, J. D. *J. Am. Chem. Soc.* **1976**, *99*, 714–718.

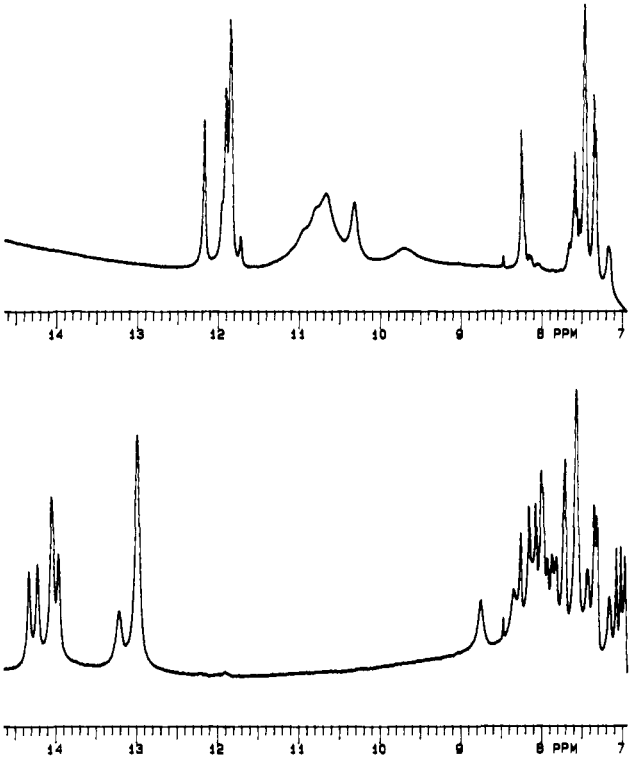


**Figure 6.** The 400-MHz $^1H$ NMR spectra at 3 °C of, upper, d[G-($^{15}N^7$)GTTTTTGG] (10.1 mM) and, lower, d[G($^{15}N^7$)GTTTTTGG]·d-[CCAAAAACC] (7.8 mM), in $H_2O/D_2O$ (9:1) containing 0.1 M NaCl, 10 mM phosphate, 0.1 mM EDTA at pH 6.9 or 7.0, respectively.

the N7 should be present. On the one hand, there is the highly structured Hoogsteen H-bonding postulated for the guanine tetrad, while, on the other hand, there is H-bonding with solvent water (hydration). However, the N7 chemical shifts observed for the tetraplex and single strand forms of **1** and **2** are strikingly similar, with the tetraplex chemical shift only slightly downfield of the single strand chemical shift. This result is consistent with a similar degree of H-bonding to the N7 in both the tetraplex and single strand forms. Further, the downfield drift of the N7 resonance as a function of increasing temperature for each of the tetraplexes, duplexes, and single strands studied here is consistent with thermal disruption of either type of H-bonding.

The accessibility of a particular N7 atom to hydration is a function of the local structure around that atom. In a duplex, the nearby base pairs will determine this local structure. Comparison of the sequences of the two duplexes studied here reveals that, while in each case the labeled N7 is in the second pair from the 5′ terminus, the flanking base pairs differ. For the **1·3** duplex the 5′ base pair is G·C, while in the **2·4** duplex the 5′ terminal pair is T·A. Terminal T·A base pairs are significantly more "open" than are terminal G·C pairs. The 1.5 ppm downfield shift of the N7 resonance in the **1·3** duplex, relative to the tetraplex or single strand forms, might be the result of more restricted hydration of the N7 in this duplex. In contrast, the identity of the N7 chemical shift in the **2·4** duplex with that in the single strand could result from a greater accessibility of the N7 to water in this frayed duplex structure, relative to the **1·3** duplex. The changes in the specific stacking interactions present may be important as well, and the $G_3$ tract present in the **2·4** duplex and the $A_5$ tract present in the **1·3** duplex also may have quite different effects on the environment at the labeled nitrogen.

## Summary

We have shown that the chemical shifts of guanine N7 atoms in two molecules which form tetramolecular complexes behave similarly and that the chemical shifts are not signal-averaged. In contrast, the chemical shifts of the same N7 atoms in the corresponding Watson–Crick duplexes show markedly different behavior. The similarity of the chemical shifts for the tetraplex and single strand structures and the difference seen for the two duplexes are consistent with the different degrees of hydrogen bonding to the N7 which could be expected in each case. Thus, although more examples will be required to establish the generality of these observations, a purine [7-$^{15}N$] label appears to be able to monitor major groove interactions, including hydration.

**Table V.** Syntheses of 1, 2, and 4

| compd[a] | scale,[b] μmole | yield,[c] μmole | av yield,[d] % | av trityl,[e] % | dA[f] | dC[f] | dG[f] | dT[f] |
|---|---|---|---|---|---|---|---|---|
| **1** | 34 | 12.1 | 88 | 95 | | | 3.9 | 5.1 |
| **2** | 33 | 10.6 | 75 | 95 | | | 3.0 | 2.0 |
| **4** | 15 | 3.0 | 67 | 91 | 2.0 | 3.0 | | |

[a] **1** is d[G($^{15}N^7$)GTTTTTGG]; **2** is d[T($^{15}N^7$)GGGT]; **4** is d-[ACCCA]. [b] Amount of support bound 3′ monomer employed. [c] Amount of pure product obtained. [d] Average actual yield per coupling step, based on the amount of material obtained after purification and on the scale of the synthesis. [e] Average of the coupling efficiencies determined by trityl assay. [f] Composition determined by enzymatic degradation and HPLC analysis.

## Experimental Section

**General Methods.** Circular dichroism spectra were obtained on a Model 60 DS Aviv spectropolarimeter. The $^1H$ and $^{15}N$ NMR spectra were recorded on Varian XL-400 or VXR-500 spectrometers. Oligonucleotide syntheses were carried out on a Milligen/Biosearch 8750 synthesizer. Reversed-phase HPLC was performed on a system consisting of a Waters 6000A pump and U6K injector, with an Autochrom CIM to allow a single pump gradient, and either a Waters 440 detector for analytical work or a Beckman 153B detector for preparative separations, using the columns indicated below.

**Synthesis and Purification of 1, 2, and 4.** The syntheses were carried out by an H-phosphonate method using a tentagel polystyrene/polyethylene glycol support[25] (**1** and **2**) or CPG (**4**) on a Milligen/Biosearch 8750 Synthesizer. The synthesis of **3** by a phosphoramidite method has been reported.[26] The crude products were purified by HPLC both before and after detritylation. The first purification used a Waters C-18 reversed-phase column (15 × 190 mm steel column or a 25 × 100 mm Radial-Pak cartridge) with a gradient of 2–40% acetonitrile/0.1 M triethylammonium acetate for **1** and a gradient of 2–50% for **2** and **4**, in 45 min at a flow rate of 4 mL/min. Detritylation was effected using 0.1 M acetic acid for 20–40 min. The second purification for **1** used a Beckman Ultrapore C-3 reversed-phase column (10 mm × 25 cm) with a gradient of 2–20% acetonitrile/0.1 M triethylammonium acetate in 45 min at a flow rate of 2 mL/min, while for **2** and **4** the C-18 column was used with a gradient of 2–20% for **4** and 2–25% for **2**. Purification of **2** was complicated by the fact that both before and after detritylation **2** elutes as two peaks. For analytical HPLC, when the fractions are warmed prior to injection, a pure sample gives only one peak, unless potassium ion is present (see supplementary material). This behavior necessitated some rechromatography to obtain pure **2**, which is reflected in the lower overall yield for this molecule. In contrast, the low yield of **4** is a result of lower coupling efficiencies using the CPG support, not purification problems. Analytical HPLC was carried out using Waters C-18 Novapak cartridges in an RCM 100 or a Beckman C-3 Ultrapore column (4.6 mm × 7.5 cm). The pure products were converted to the sodium or potassium forms by ion exchange using sodium or potassium form Bio-Rad AG50W-X4 resin, after HPLC using a C-18 column with acetonitrile and 0.1 M ammonium bicarbonate to remove all triethylammonium acetate. The ratio of monomers produced upon enzymatic degradation of the purified molecules was determined by integration of the peaks obtained by HPLC on the Waters C-18 Novapak column using Baseline chromatography software. The results of the syntheses are summarized in Table V. Chromatograms of **1**, **2**, and **4** after purification are available as supplementary material.

**Acknowledgment.** This work was supported by grants from the National Institutes of Health (GM31483) and the Busch Memorial Fund and an American Cancer Society Faculty Research Award to R.A.J.

**Supplementary Material Available:** Portions of the 500-MHz $^1H$ 2D NOESY contour plots of d[G($^{15}N^7$)GTTTTTGG] (**1**) and d[T($^{15}N^7$)GGGT] (**2**) and HPLC analyses of **1**, **2**, and **4**, after purification (3 pages). Ordering information is given on any current masthead page.